Experimental Investigations of Liquid Oxygen/Methane Combustion at Very Low Mixture Ratio at the Mascotte Test Facility

Lucien Vingert, Nicolas Fdida, Yves Mauriot, Ismael Ortega Colomer, Cornelia Irimea, David Delhaye, Ajmal Khan Mohamed, Vincent Corbas, Marie Theron

Experimental Investigations of Liquid Oxygen/Methane Combustion at Very Low Mixture Ratio at the Mascotte Test Facility.

By Lucien VINGERT,[1)] Nicolas FDIDA,[1)] Yves MAURIOT,[1)] Ismael ORTEGA COLOMER,[1)] Cornelia IRIMEA,[1)] David DELHAYE,[1)] Ajmal Khan MOHAMED,[1)] Vincent CORBAS,[1)] and Marie THERON [2)]

[1)]*ONERA The French Aerospace Lab, Université Paris Saclay, Palaiseau, France*
[2)]*CNES, Launcher Directorate, Paris, France*

A short test series was run on the Mascotte cryogenic test facility of Onera, with the objective to demonstrate the feasibility of applying several diagnostics to the characterization of liquid oxygen/methane combustion in the range of low mixture ratios typical of gas generator operation. Tunable diode laser absorption spectroscopy and emission spectroscopy were used to investigate the gas mixture in the near injector region, while particle sampling was applied to the characterization of soot.

Key Words: Oxygen/methane combustion, TDLAS, soot measurement

Nomenclature

P	:	pressure, MPa
T	:	temperature, K
O/F	:	mixture ratio
J	:	momentum flux ratio
Subscripts		
LOX	:	liquid oxygen
CH_4	:	methane

1. Introduction

Various considerations, including ambitious goals like interplanetary journeys to Mars, but also international competition resulting in the need of reusability and drastic cost reduction objectives, make it highly probable that the next generation of launchers will be propelled with methane instead of hydrogen as a fuel, especially if its main advantages are taken into account. Indeed, the liquefaction temperature of methane around 100 K, close to the oxygen's one, makes it much easier to handle than hydrogen which has to be stored at temperatures as low as 20 K. Secondly, the density of liquid methane is six times higher than the liquid hydrogen's one, which enables a significant reduction of the tank's volume and mass. These advantages make methane still competitive despite the slight loss in specific impulse of oxygen/methane compared to oxygen/hydrogen propellants combination.

In this context, the development of a new generation of engines propelled by liquid oxygen (LOX) and methane (CH_4) for reusable launchers has recently started within ESA's FLPP NEO program, resulting in new needs for characterization of LOX/CH_4 combustion in operating conditions representative of rocket-engine combustion devices. Indeed, methane or natural gas is certainly a common fuel, used in many domestic applications, so that its combustion may be considered as well known, and that no peculiar difficulty should be expected when enforcing it instead of hydrogen in cryogenic rocket engines. The reality is however somewhat different. The problem is that even if the combustion of methane in air is extensive and well characterized, it is not the case for methane with pure oxygen, in particular when they are both injected at cryogenic temperatures and at high pressure. Kinetic schemes, reduced to be convenient in numerical simulation codes, become available,[1)] but they have to be validated. Moreover, gas generators of cryogenic rocket engines operate in extremely unusual conditions: on one hand, both propellants are cryogenic liquids that have to be atomized, vaporized and well mixed, and on the other hand, the mixture ratio is very low, typically in the range of 0.25 to 0.50. These very specific and totally unusual combustion regime exhibit several difficulties and peculiar features that justify dedicated research activities, such as single element tests that were recently run at the Mascotte test facility of ONERA in the framework of the CNES/ONERA R&D program. The Mascotte research test bench enables the use of methane as a fuel, in gaseous or in liquid phase, since the beginning of the 2000s.[2,3)]

During a test campaign run in 2018, four operating points, ranging from sub- to supercritical pressures (2.5 to 6.0 MPa), were operated and characterized during the stabilized phase, in a single injector element configuration with optical access.[4)] In order to be fully representative of a gas generator, both propellants were injected at cryogenic temperature, i.e. in liquid or transcritical phase.

The structure of the spray and the surrounding flame were investigated with high speed cameras in the ultraviolet and visible domains. The experimental setup was similar to the one used previously in the CNES-ArianeGroup-ONERA-EM2C R&D consortium where both oxygen/methane and oxygen/hydrogen conditions were tested.[5,6)] But there arose a

first problem: a cloud of unidentified dense fluid appeared around the burning spray (Fig. 1). This makes the post-processing of the images very tricky. An Abel transform of the OH* radical emission images to determine the flame angle and anchoring, as well as the analysis of shadowgraphs or Schlieren images to determine the penetration length of the LOX jet, may induce incorrect conclusions.

Fig. 1. Liquid oxygen / liquid methane flame produced by a single element coaxial injector.

Those many unexpected and underestimated difficulties encountered in the previous tests motivated the development and the implementation of dedicated experimental techniques. Therefore, we decided to reduce our ambitions and to returned to less severe conditions which imply: a lower pressure and a more classical liquid oxygen / gaseous methane injection. We installed diagnostics that were never applied to Mascotte previously, with the objective to evaluate their abilities to investigate several phenomena linked to this peculiar situation and to improve/adapt them before going back to operating conditions representative of the real working regimes. Tunable diode laser absorption spectroscopy (TDLAS) and emission spectroscopy were used to investigate the gas mixture in the near injector region, while particle sampling was applied to the characterization of soot.

2. Experimental set-up

Figure 2 shows the high pressure combustion chamber with optical access operated on the Mascotte test bench for these tests. The TDLAS line of sight was on the upper corner of the window, in the recirculation zone around the flame of Fig. 1.

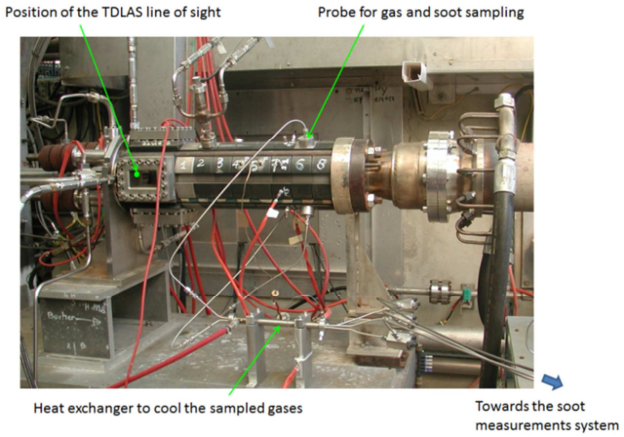

Fig. 2. Experimental set-up : single injector combustion chamber with optical access and gas sampling probes.

The gas and soot sampling probes were located in the downstream part of the chamber, in a section were the combustion is supposed to be complete and the gaseous mixture homogeneous. The same experimental set-up was already used in previous experiments run in the same range of mixture ratios in the 2000s for visualization, temperature measurements and gas sampling tests. [5,8)]

The diameters of the shear coaxial injector were chosen in order to maintain an acceptable momentum flux ratio at injection (J between 5 and 25). The propellants temperatures were approximately T_{LOX} = 85 K (subcooled liquid oxygen) and T_{CH4} = 298 K (ambient temperature gaseous methane).

3. Spectroscopic investigations of the gaseous mixture

3.1. Emission spectrum of the flame

The emission spectrum of the flame was recorded between 188 nm and 860 nm with an Ocean Optics S2000 spectrometer, with a resolution of 0.37 nm and an exposure time of about 100 ms. Light coming from the flame was collected by a lens focused on the flame axis, approximately in the middle of the window section. Flame emission spectroscopy was used to identify the most emitting chemical species for each operating condition. Figure 3 shows the emission spectra of the flame for two pressure conditions (0.45 MPa and 0.9 MPa in red and blue respectively).

The emission spectra of the flame are consistent with the results of Lux and Haidn who also studied the emission spectrum of high-pressure LOX/CH_4 flames.[7)] The intense emission peak observed around 310 nm is due to the presence of the OH radical whereas the other prominent peak around 430 nm is due to CH. Both radicals are known to be produced by combustion in the chemical reaction zone. Other species, such as C_2 are identified by several small peaks, called Swan bands, in the case of the 0.45 MPa spectrum only. In the case of the 0.9 MPa spectrum, the continuous emission background, which can be attributed to larger molecules such as CO_2, between 350 nm and 650 nm, is too intense to see the Swan bands in this operating condition. In both pressure cases, OH and CH are intense enough to come out of the background and could be used as markers of the reaction zone for imaging purpose.

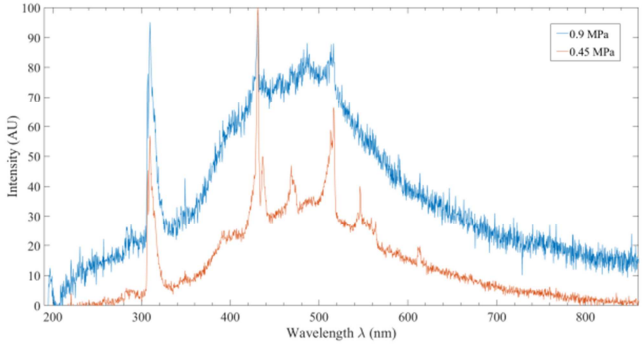

Fig. 3. Emission spectra of the LOX/CH_4 flame.

3.2. TDLAS measurements

Tunable diode laser absorption spectroscopy [9] has been used to characterize H_20 vapor concentration, temperature and pressure in the upstream, near injector region, of the combustion chamber but outside of the burning jet. The goal was to check the feasibility of this technique in high pressure conditions (up to 6 MPa) and water vapor behavior in the recirculation zone around the flame. The TDLAS instrument is built around a diode laser emitting around 1.39 µm enabling the probing of several H_20 absorption lines with intensities easily detectable in Mascotte conditions and having no interference with lines from other species. At these wavelengths, a diode laser from telecom technology can be used. We chose a module from the EBLANA manufacturer incorporating a diode laser and all the electronics to control its current and temperature which therefore needs only a voltage ramp to tune the laser emission on a spectral interval of about 5 cm^{-1}. Figure 4 shows the H_20 lines which can be addressed when spectral tuning is checked with the laser beam crossing a 10 cm long gas cell filled with water vapor at the pressure of 100 mbar and at 300 K.

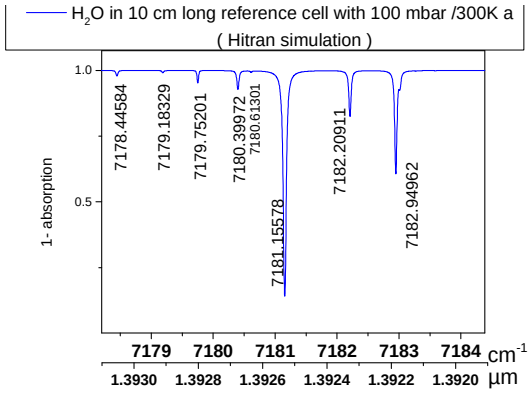

Fig. 4. Spectral window coverage of the Eblana diode laser showing addressed H_2O absorption lines (spectrum acquired in a reference gas cell 10 cm long and filled with H_2O at a pressure of 100 mbar and at 300 K).

In this telecom domain, optical fibers and couplers can be used from the diode laser up to the test section. Part of the beam is sampled to feed a fibered Faby Perot and to cross a reference gas cell for spectral calibration as shown in Fig. 5.

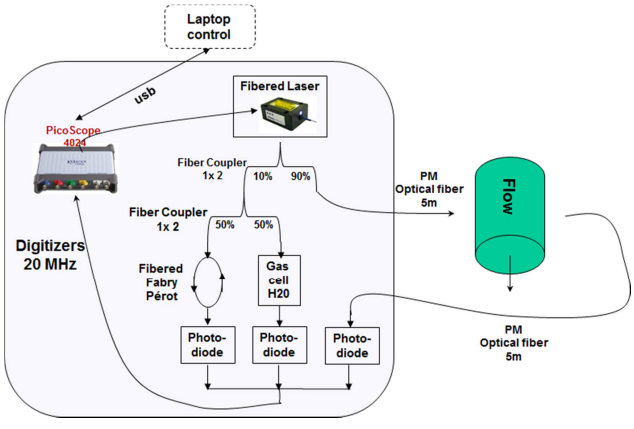

Fig. 5. Components of the TDLAS spectrometer.

Laser intensities for the three channels are measured by amplified InGaAs photodiodes whose output electric signals are digitized by a high speed digitizer, the Picoscope 4824 model from the PicoWave manufacturer (four channels with sampling rate up to 20 MHz on 12 bits over a memory of 107 samples per channel). For the channel crossing the test section, an optical fiber brings the laser beam up to an optical collimator touching the test section optical window. Careful orientation of this collimator directs the laser beam to cross the test section and to point onto another collimation focusing light in a fiber optic which brings the final beam on a photodiode inside the spectrometer. All elements of the spectrometer are stacked in a 3U 19 inch rack and the whole system is controlled by a laptop via an in-house LabView software.

Spectra acquisition frequency must be set high enough to temporally 'freeze' the turbulence, thereby avoiding spectrum envelope deformation. For these experiments, the maximum frequency of 12.5 kHz (limited by laser electronics and detector amplifier bandwidths possibilities) has been chosen and Fig. 6 presents an example of successive spectra acquired during one of the Mascotte runs.

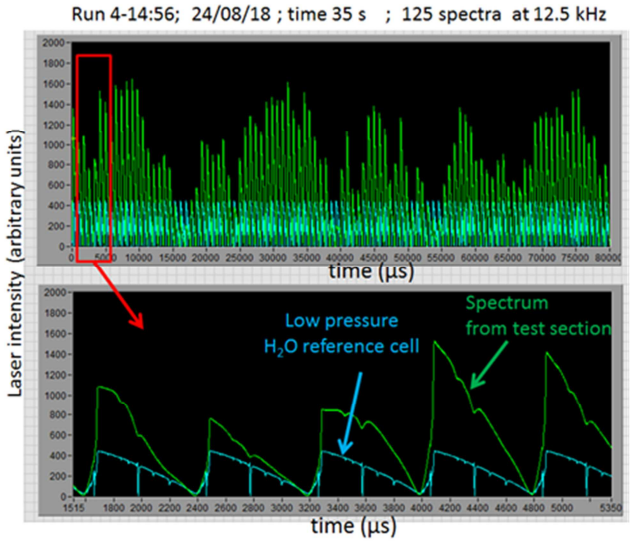

Fig. 6. One hundred successive spectra during a Mascotte run (taken at half run time).

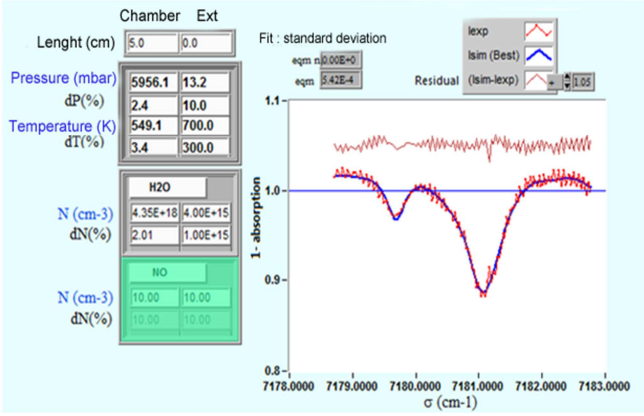

Fig. 7. Example of spectrum inversion.

The spectra still present some slight deformations of the envelope but the absorption lines are perfectly visible and exploitable to extract the thermodynamic parameters of the gaseous medium crossed by the laser beam.

Some of the spectra are also quite attenuated but they can nevertheless be processed with the inconvenient of having lower accuracies for the extracted parameters.

Acquisition memory limitations led us to acquire sets of 125 spectra at 12.5 kHz (set duration of 10 ms) repeated every one second in order to sample the whole run duration of 120 s.

The data processing, also performed via a LabView software (Fig. 7), consists in inverting each spectrum to deliver H_20 concentration, temperature and pressure, which are plotted for each series as shown in Fig. 8.

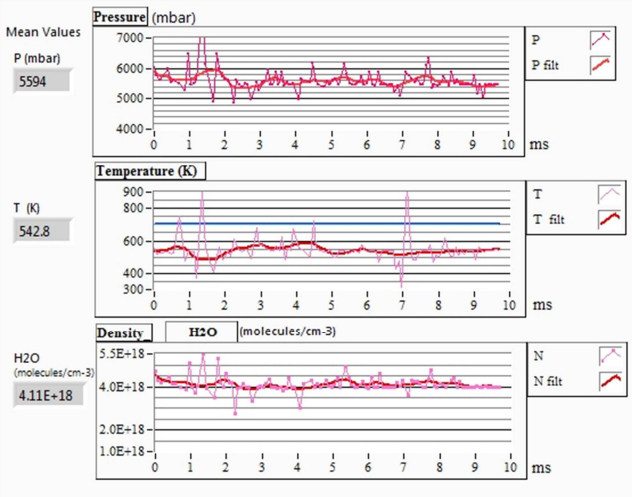

Fig. 8. Time evolution of different parameters for a set of 125 successive spectra.

The average values for each set are taken as the final experimental data, which are to be compared to results from other instruments (pressure sensor and thermocouples). Examples of such comparisons are shown in Fig. 9 and Fig.10 for a run at medium pressure around 0.5 MPa. During this test, three different mixture ratios of 0.97, 079 and 0.64 were achieved for 20 s each. Some instabilities were observed but studying these phenomena is not in the purpose of the present study; they are therefore not discussed here.

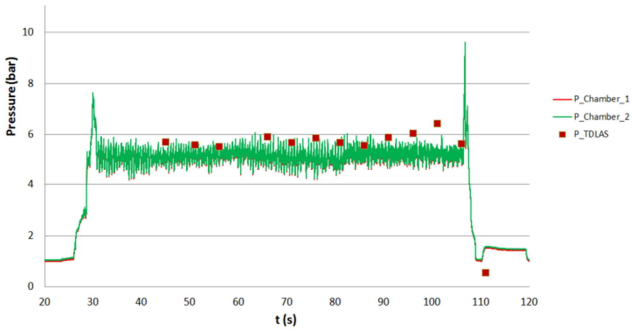

Fig. 9. Comparison of TDLAS measurements to values provided by classical pressure sensors.

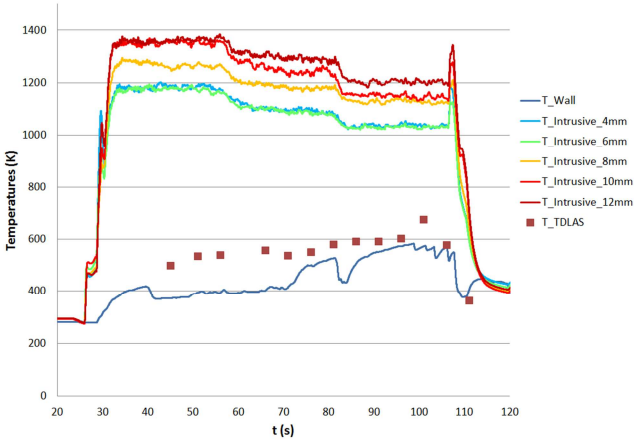

Fig. 10. Comparison of TDLAS measurements to values provided by thermocouples.

The TDLAS pressure values correlate well with those from the pressure sensors. The comparison of the TDLAS temperature values with thermocouple measurements is not so straight forward because the TDLAS line of sight was located in the upper corner of the window, in the recirculation zone around the flame. The temperature of this region is much lower than the temperature of the downstream part of the chamber, as indicated by the intrusive thermocouples. The latter were implemented in the module n°7 of Fig. 2. Finally, the only thermocouple measurement that compares with the TDLAS is the one which was implemented on the bottom dummy window at roughly the same axial distance from the injector than the TDLAS.

For higher pressures around 6 MPa, no significant absorption lines were found in the spectra. Absorption spectra simulations (Fig. 11) at these pressure levels show a quite important line broadening, which hinders the identification of absorption lines in the spectral window covered by our experiments.

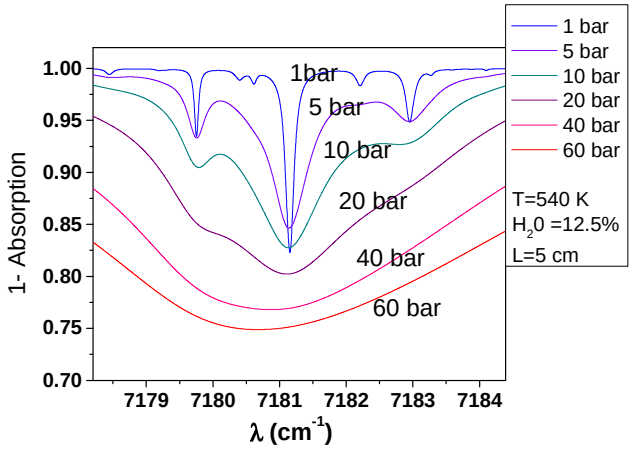

Fig. 11. Simulations of absorption line pressure broadening.

Spectrum simulations over a wider spectral domain as shown in Figure 12 lead us to conclude that a laser with a very broadband spectral window is needed to acquire such high pressure broadened absorption lines.

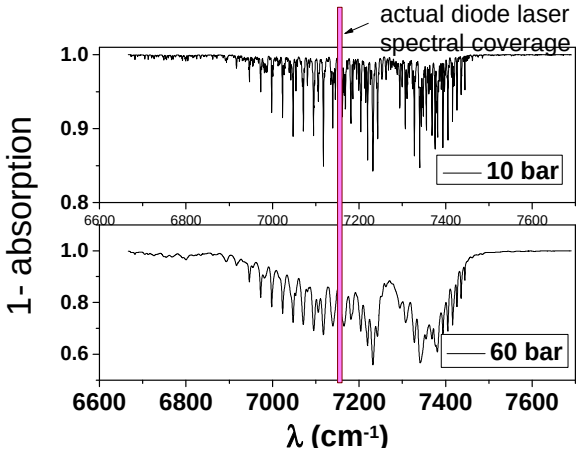

Fig. 12. Spectral simulations over a wider spectral band encompassing a whole vibrational band of H_20.

4. Soot characterization

The experimental configuration used for the measurement of soot emissions from the combustion chamber, usually used for the characterization of aircraft engines exhaust,[10] is depicted in Fig. 13. N.B.: the apparatus schematized here is located downstream of the arrow on bottom right of Fig. 2.

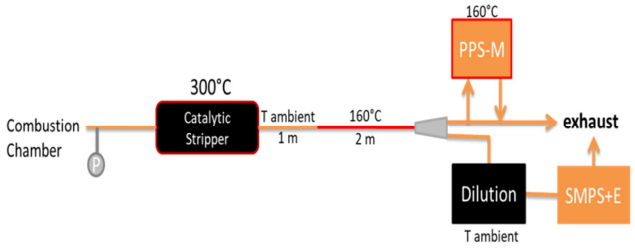

Fig. 13. Schematic representation of the sampling line implemented for soot measurements.

Firstly, the pressure at the line inlet was measured to ensure the integrity of the measurement instruments. After the pressure measurement, the sample flow was conducted through a catalytic stripper heated at 300 °C to remove the particle and gas-phase semi-volatile fraction potentially present in the sample. The sampled flow was then lead to the measurement instruments with a metallic sampling line where the first meter was at ambient temperature and the two following meters were heated to 160 °C. Finally the sample flow was driven by a two way flow splitter. The first part was driven to a Pegasor Particle Sensor type M (PPS-M) heated at 160°C to measure the particle number and mass. The second part was diluted at ambient temperature and then analyzed using a Scanning Mobility Particle Sizer coupled to a Faraday cup electrometer (SMPS+E) to determine the particle size distribution.

The system was tested during different runs to optimize the setup. Finally, exploitable results were obtained during a final run operated at a pressure of 0.85 MPa, and an O/F mixture ratio of 0.58 (the run lasted 70 seconds).

Figure 14 shows the evolution of particle number and mass along the run. As can be seen on Fig. 14, there was some instability in the signals during the first part of the run. This instability disappeared at 50 s after the beginning of the run (20 s after ignition). This might be linked to instabilities in the combustion chamber. After stabilizing the combustion conditions, the particle concentration was 4.01 10^7 ± 0.38 10^7 particles per cm^3 and the mass concentration was 8.35 ± 0.79 mg/m^3.

The size distribution of the particles was measured between 5.6 nm and 90.2 nm with a resolution of 32 size bins. It is worth noticing that what is actually measured is the electrical mobility diameter. Figure 15 shows the size distribution obtained during the run. It appears to be bi-modal, with a shoulder around 50 nm. Table 1 summarizes the statistics from the size distribution. The definitions and physical meaning of the provided characteristic values can be found in Ref.11).

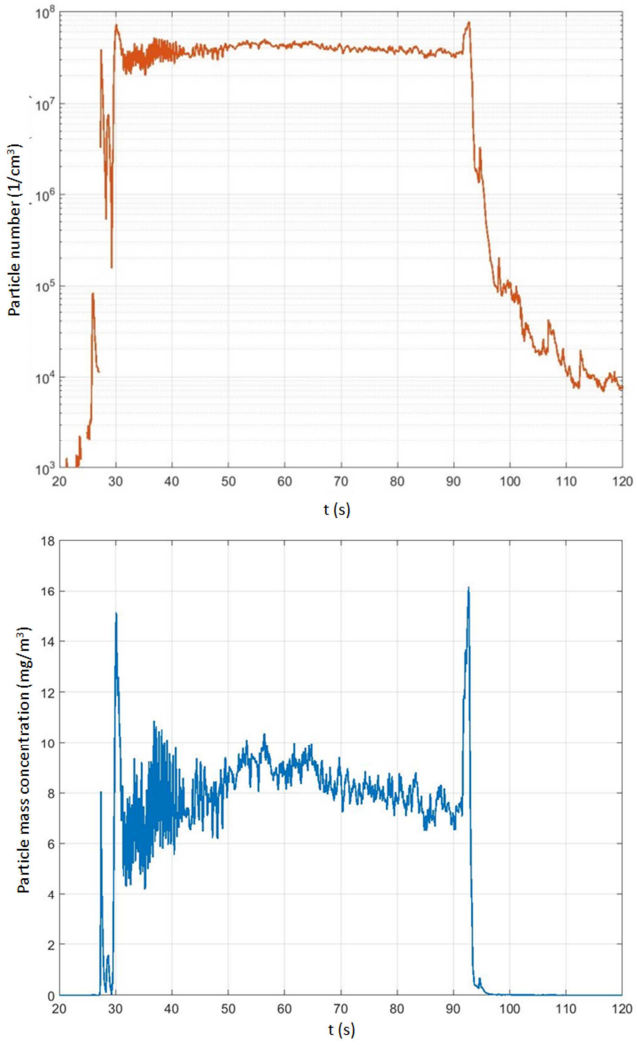

Fig. 14. Particle number (top) and mass concentration (bottom) values during a test at P = 0.85 MPa and O/F = 0.58

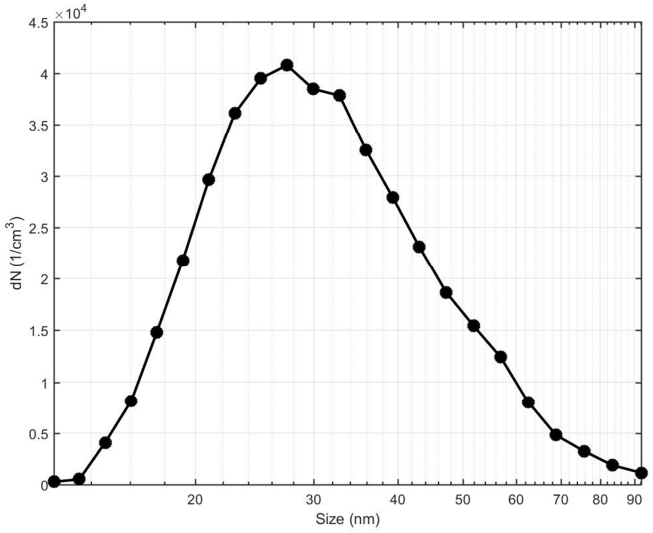

Fig. 15. Particle size distribution obtained during the test run.

Table 1. Statistics of the size distribution.

Characteristic diameters	Values
Geometric mean diameter	28.72 (nm)
Median	27.40 (nm)
Mode	27.30 (nm)
Arithmetic mean diameter	31.48 (nm)
Geometric standard deviation	1.56

Since the distribution obtained was bimodal, it was fitted to obtain the maximum information possible. We used two lognormal functions to fit the obtained size distribution (Fig 16). As can be seen, we found two modes, the first one centered at 24.40 nm and the second one at 36.79 nm.

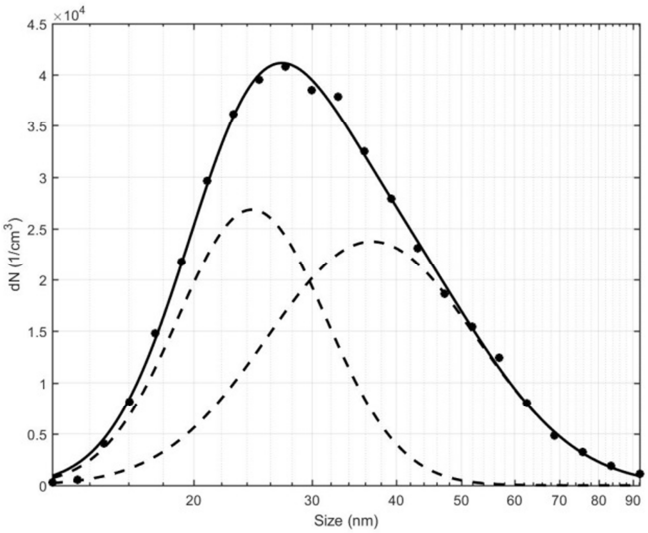

Fig. 16. Fitted size distribution.

7. Conclusion

This work presented insights into the characteristics of cryogenic combustion of liquid oxygen/methane performed on the Mascotte test rig. The novelty of this work relied on the implementation of optical in-situ diagnostics coupled with ex-situ techniques performed on the sampled exhaust for extreme combustion conditions.

A general overview of the main molecular species present in these combustion conditions was given by emission spectroscopy measurements.

Simultaneously detailed experiments proved that TDLAS can be used in the Mascotte test rig for an in depth characterization, at least at moderate pressure. This technique provided valuable information about the temperature, pressure and molecular species concentration values inside the combustion chamber in a non-intrusive way. Further improvements of the TDLAS technique are nevertheless necessary to apply it at higher pressure. They mainly consist in using wide spectral band lasers, better coupling to the test section, purging of atmospheric water vapor, and applying higher spectrum acquisition frequency in order to better ‘freeze‘ turbulence. In parallel, a tomographic version of TDLAS using multiple coupled laser beams and/or beam scanning is also under development to enable local values and spatial resolution instead of only line of sight integrated values. [12)]

Furthermore, these experiments provided a first characterization of soot particles produced in these specific combustion conditions. The set-up was optimized in order to have access to soot particles mobility diameters, mass concentrations and numbers in the short time available during each run. The obtained data can be used to deduce the radiative properties of soot particles in the combustion chamber or to provide indirect information on the combustion processes by comparing the obtained physical properties of soot particles with the ones obtained in well characterized combustion conditions of CH_4.

Nevertheless, these preliminary tests were conducted in simplified conditions, i.e. at moderate pressure, at mixture ratios slightly higher than the range of interest and with gaseous methane injected at room temperature instead of liquid or transcritical methane. Further experiments with more realistic gas generator operating conditions are foreseen and they will benefit from the implemented diagnostics and additional optical techniques in development.

References

1) Zhukov, V.P. and Kong, A.F.: A compact reaction mechanism of methane oxidation at high pressures, *Progress in Reaction Kinetics and Mechanism* **43,** (2018), pp. 62-78.
2) Vingert, L., Habiballah, M., and Vuillermoz, P.: Upgrading of the Mascotte cryogenic test bench to the LOX/Methane combustion studies, 4th International Conference on Launcher Technology, Liège, Belgium, 2002.
3) Vingert, L., Ordonneau, G., Fdida, N. and Grenard, P.: A rocket under a magnifying glass, Challenges in Combustion for Aerospace Propulsion, *Journal of Aerospace Lab* **11**, (2016), chapt. 15.
4) Théron, M., Martin Benito, M.,Vieille, B., Vingert, L., Fdida, N., Mauriot, Y., Blouquin, R., Seitan, C., Onori, M., and Lequette, L.: Experimental and numerical investigation of LOX/Methane Cryotechnic Combustion at low mixture ratio, 8th EUCASS, Madrid, Spain, 2019.
5) Singla, G. et al.: Transcritical oxygen / transcritical or supercritical methane combustion, *Proceedings of the Combustion Institute* **30**, (2005).
6) Fdida, N., Vingert, L., Ordonneau, G., and Petitot, S.: Coupling high-speed imaging diagnostics to study a LOX/GH2 flame in a high-pressure rocket combustor, 5th EUCASS, Munich, Germany, 2013.
7) Lux, J., and Haidn, O.: Flame Stabilization in High-Pressure Liquid Oxygen/Methane Rocket Engine Combustion, *Journal of Propulsion and Power*, Vol.**25**, Issue 1, (2009), pp.15-23.
8) Vingert, L.: Rapport d'essais Mascotte. Campagne de prélèvements de gaz., ONERA RT 1/09670, 2004 (in French).
9) Mohamed, A.K., and Lefebvre, M.: Laser absorption spectroscopy to probe chemically reacting flows, *AerospaceLab Journal* **1**, *(2009).*
10) Ortega, I.K., Delhaye, D., Ouf, F.X., Ferry, D., Focsa, C., Irimiea, C., Carpentier, Y., Chazallon, B., Parent, P., Laffon, C., Penanhoat, O., Harivel, N., Gaffié, D., and Vancassel X.: Measuring non-volatile particle properties in the exhaust of an aircraft engine. *AerospaceLab Journal* **11**-08, (2016), chapt. 8.
11) Grainger, R.G.: Some useful formulae for aerosol size distributions and optical; properties, 2017, http://eodg.atm.ox.ac.uk/user /grainger/ research/aerosols.pdf (accessed February 2019)
12) Corbas, V., Champagnat, F., Le Besnerais, G., Vincent -Randonnier, A., and Mohamed, A.K.: Mapping of H2O concentration and temperature in a turbulent methane/air diffusion flame using multispectral absorption tomography, 7th EUCASS, Milano, Italy, 2017.